DESIGN OF A MOLECULAR EXCHANGE-BASED ROBUST PERCEPTRON FOR BIOMOLECULAR NEURAL NETWORK

Moshiur Rahman*, **Muhtasim Ishmum Khan*** **& Md. Shahriar Karim**†
Department of Electrical and Computer Engineering
North South University, Dhaka, Bangladesh
{moshiur.rahman21,muhtasim.ishmum,shahriar.karim}@northsouth.edu

ABSTRACT

A molecular perceptron is of immense interest due to its computing and classification ability in biophysical and aqueous environments. Because such a perceptron relies on biochemical interactions, it must adapt to perturbations and be resilient against stochastic fluctuations to maintain faithful *in vivo* classification. In this paper, we design a molecular exchange mechanism (MEM)-based perceptron following a set of evolutionarily preserved *in vivo* signaling steps, including negative feedback known for noise regulation. The efficacy study of the MEM-perceptron demonstrates an improved adaptation against perturbations and noise.

1 INTRODUCTION

The basic building block of a biomolecular neural network (BNN) is the molecular perceptron that resembles activation functions by chemical interactions (Hjelmfelt et al., 1991). Such BNN-based molecular machines are suitable in applications ranging from point-of-care disease detection to smart drug delivery (Lopez et al., 2018; Ma et al., 2022), and can be implemented using DNA strands as the interacting species (Qian et al., 2011; Cherry & Qian, 2018). A molecular perceptron design often uses a deterministic analysis approach involving Ordinary Differential Equations (ODE) and mass-action kinetics to form a solid theoretical cue for general computing (Bournez et al., 2017). For instance, previous studies used molecular sequestration (Moorman et al., 2019) and phosphorylation-dephosphorylation (Samaniego et al., 2021), which followed deterministic ODE formulation in perceptron design. In many BNN applications, the molecular mixture of species is subdivided into smaller compartments, each with considerably low-concentration molecular interactions making intrinsic noise inherent in the system (Plesa et al., 2018). Due to noise, the deterministic steady state concentration may deviate from its acceptable threshold, causing the perceptron to be error-prone. In contrast to its detrimental role, evidence also suggests noise as a sensitivity enhancer (Gammaitoni et al., 1998), frequently observed in many species (Douglass et al., 1993; Ozbudak et al., 2002). An intriguing question thus arises, whether a mechanism can curb noise to an acceptable range and still perform as a molecular perceptron. As a solution, we propose a model

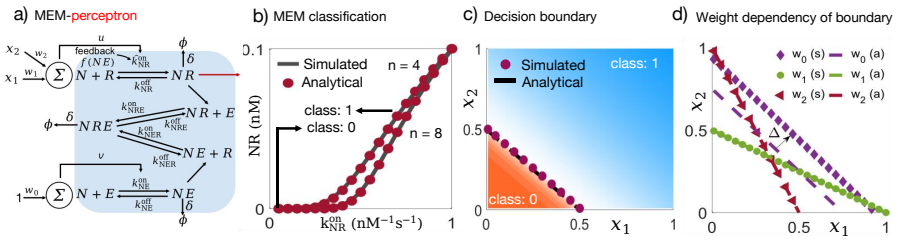

Figure 1: a) Molecular exchange mechanism: Besides a direct path, NR forms via NRE. b) ReLU formation by NR for different strengths n of feedback of NE. c) Decision boundary for 0 and 1 class. d) Boundary shift for weight variations $[w_0\ w_1\ w_2]$, (s): simulated, (a): analytical.

*Equal contribution
†Corresponding author

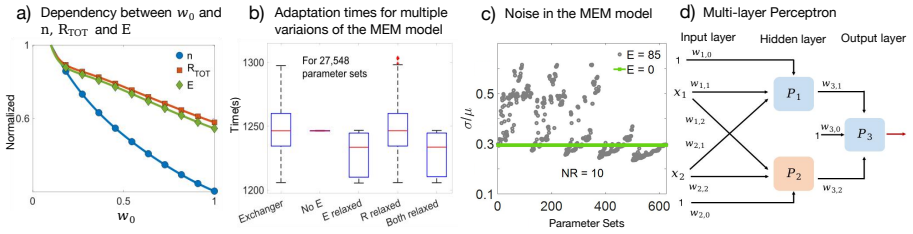

Figure 2: a) Change in n, R_{TOT} and E for different values of w_0 to eliminate Δ. b) Adaptation time for production perturbations of N. c) Presence of E reduces the CV for favored kinetics. d) Multilayer MEM-perceptron network, capable of performing non-linear classification.

comprised of molecular interactions seen in many biophysical contexts (Umulis et al., 2009; Papouin et al., 2012) that confer perceptron-like behavior while maintaining an improved noise control.

2 Methods and Results

MEM Model: The MEM-perceptron performs binary classification for inputs x_1, x_2 using the species NR (Fig. 1a,b,c). The classification boundary follows the decision boundary equation, defined as $x_2 = -(w_1/w_2)x_1 + (w_0/w_2)$, for w_1, w_2 variations, whereas variations in w_0 produce a deviation Δ(Fig. 1d, 2a), traceable through Ω. The MEM-perceptron considers mass-action based ODEs, and the steady state value of NR provides its decision boundary (Appendix A.2).

$$
\begin{aligned}
&\frac{d}{dt}[NR] = \hat{k}^{\text{on}}_{\text{NR}}[N][R] + k^{\text{off}}_{\text{NRE}}[NRE] - k^{\text{off}}_{\text{NR}}[NR] \\
&- k^{\text{on}}_{\text{NRE}}[NR][E] - \delta[NR] \\
&\frac{d}{dt}[NE] = k^{\text{on}}_{\text{NE}}[N][E] + k^{\text{off}}_{\text{NER}}[NRE] - k^{\text{off}}_{\text{NE}}[NE] \\
&- k^{\text{on}}_{\text{NER}}[NE][R] - \delta[NE] \\
&\frac{d}{dt}[NRE] = k^{\text{on}}_{\text{NRE}}[NR][E] + k^{\text{on}}_{\text{NER}}[NE][R] - k^{\text{off}}_{\text{NRE}}[NRE] \\
&- k^{\text{off}}_{\text{NER}}[NRE] - \delta[NRE]
\end{aligned} \tag{1}
$$

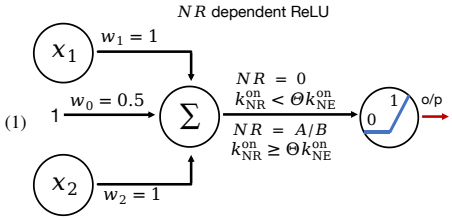

$$
[NR] \approx \begin{cases} \underbrace{(\beta k^{\text{on}}_{\text{NR}} r[N] - k^{\text{on}}_{\text{NE}}[N] + [NE](\gamma r k^{\text{on}}_{\text{NR}}))}_{\text{A}} \Big/ \underbrace{\gamma k^{\text{on}}_{\text{NE}}}_{\text{B}} & \text{if } \underbrace{w_1 x_1 + w_2 x_2}_{k^{\text{on}}_{\text{NR}}} \geq \Omega \underbrace{w_0}_{k^{\text{on}}_{\text{NE}}} \\ 0 & \text{if } w_1 x_1 + w_2 x_2 < \Omega w_0 \end{cases} \tag{2}
$$

Enhanced adaptation to perturbation: An enhanced chemical adaptation ability increases the fidelity of the perceptron outcomes in the presence of production perturbations of the interacting species. We compare different candidate MEM models to assess the adaptability (Fig. 2b) and choose the model that minimizes adaptation time.

Reduced noise: For noise analysis, we numerically approximate the Chemical Master Equation (CME)(Van Kampen, 1992) using Gillespie's algorithm (Gillespie, 1976). A numerical screen over parameter sets of NRE formation demonstrates kinetics-dependent noise control (Fig. 2c) quantified by the coefficient of variation (CV) reduction of the steady state NR count (Appendix A.4).

3 Discussion

The designed MEM-perceptron includes feedback circuitry and demonstrates an enhanced adaptation against perturbations. It is also resilient against stochastic fluctuations needed for molecular computing (Plesa et al., 2018). Interestingly, noise injection during artificial neural network training regularizes the network (Bishop, 1995). As the MEM-perceptron demonstrates improved noise control, a multilayer network consisting of MEM-perceptron may be more flexible to noise addition at low-concentration molecular interactions. Aligned with the previous studies, the MEM-perceptron is scalable to form multilayer perceptron (MLP) (Fig. 2d) for a chosen set of weights (w_i) ensuring that each module works independently as a perceptron. Overall, the ability of the MEM-perceptron to maintain the decision threshold within an acceptable range and a potential regularizing role with an improved noise control make it a viable avenue to explore for BNN applications.

URM STATEMENT

The authors acknowledge that at least one key author of this work meets the URM criteria of ICLR 2024 Tiny Papers Track.

REFERENCES

David F Anderson, Badal Joshi, and Abhishek Deshpande. On reaction network implementations of neural networks. *Journal of the Royal Society Interface*, 18(177):20210031, 2021.

Chris M Bishop. Training with noise is equivalent to tikhonov regularization. *Neural computation*, 7(1):108–116, 1995.

Olivier Bournez, Daniel S Graça, and Amaury Pouly. Polynomial time corresponds to solutions of polynomial ordinary differential equations of polynomial length. *Journal of the ACM (JACM)*, 64 (6):1–76, 2017.

Kevin M Cherry and Lulu Qian. Scaling up molecular pattern recognition with dna-based winner-take-all neural networks. *Nature*, 559(7714):370–376, 2018.

Daniel Choquet and Antoine Triller. The dynamic synapse. *Neuron*, 80(3):691–703, 2013.

John K Douglass, Lon Wilkens, Eleni Pantazelou, and Frank Moss. Noise enhancement of information transfer in crayfish mechanoreceptors by stochastic resonance. *Nature*, 365(6444):337–340, 1993.

Luca Gammaitoni, Peter Hänggi, Peter Jung, and Fabio Marchesoni. Stochastic resonance. *Reviews of modern physics*, 70(1):223, 1998.

Daniel T Gillespie. A general method for numerically simulating the stochastic time evolution of coupled chemical reactions. *Journal of computational physics*, 22(4):403–434, 1976.

Allen Hjelmfelt, Edward D Weinberger, and John Ross. Chemical implementation of neural networks and turing machines. *Proceedings of the National Academy of Sciences*, 88(24):10983–10987, 1991.

Shahriar Karim, Gregery T Buzzard, and David M Umulis. Efficient calculation of steady state probability distribution for stochastic biochemical reaction network. *BMC genomics*, 13(6):1–11, 2012.

Randolph Lopez, Ruofan Wang, and Georg Seelig. A molecular multi-gene classifier for disease diagnostics. *Nature chemistry*, 10(7):746–754, 2018.

Qian Ma, Mingzhi Zhang, Chao Zhang, Xiaoyan Teng, Linlin Yang, Yuan Tian, Junyan Wang, Da Han, and Weihong Tan. An automated dna computing platform for rapid etiological diagnostics. *Science Advances*, 8(47):eade0453, 2022.

Andrew Moorman, Christian Cuba Samaniego, Carlo Maley, and Ron Weiss. A dynamical biomolecular neural network. In *2019 IEEE 58th conference on decision and control (CDC)*, pp. 1797–1802. IEEE, 2019.

Ertugrul M Ozbudak, Mukund Thattai, Iren Kurtser, Alan D Grossman, and Alexander Van Oudenaarden. Regulation of noise in the expression of a single gene. *Nature genetics*, 31(1):69–73, 2002.

Thomas Papouin, Laurent Ladépêche, Jérôme Ruel, Silvia Sacchi, Marilyne Labasque, Marwa Hanini, Laurent Groc, Loredano Pollegioni, Jean-Pierre Mothet, and Stéphane HR Oliet. Synaptic and extrasynaptic nmda receptors are gated by different endogenous coagonists. *Cell*, 150(3): 633–646, 2012.

Tomislav Plesa, Konstantinos C Zygalakis, David F Anderson, and Radek Erban. Noise control for molecular computing. *Journal of the Royal Society Interface*, 15(144):20180199, 2018.

Lulu Qian, Erik Winfree, and Jehoshua Bruck. Neural network computation with dna strand displacement cascades. *nature*, 475(7356):368–372, 2011.

Christian Cuba Samaniego, Andrew Moorman, Giulia Giordano, and Elisa Franco. Signaling-based neural networks for cellular computation. In *2021 American Control Conference (ACC)*, pp. 1883–1890. IEEE, 2021.

David Umulis, Michael B O'Connor, and Seth S Blair. The extracellular regulation of bone morphogenetic protein signaling. *Development*, 136(22):3715–3728, 2009.

Nicolaas Godfried Van Kampen. *Stochastic processes in physics and chemistry*, volume 1. Elsevier, 1992.

A Appendix

A.1 Details of the MEM-perceptron design

The molecular exchange mechanism (MEM) is similar to interactions commonly seen in various biophysical systems, for example, in the synaptic cleft of the brain (Fig. 4a). There are three species working in the MEM: N (signaling agent, which could be a neurotransmitter), R (receptor), and E (exchanger molecule). The molecular exchange between the species occurs with the help of the exchanger molecule. Production of the decision-making species NR occurs in two channels. Firstly, NR is produced from the interaction between N and R. Secondly, the exchange of E between NRE and NR contributes to NR production. The exchanger molecule E also facilitates the production of the species NE which is used to impose negative feedback on the forward production rate of NR, leading to a smooth ReLU-like behavior of NR in steady state, similar to Anderson et al. (2021). As molecular production adds noises, the designed dynamics takes N and E as a constant source to establish a better control over noise. A conservation condition for R is maintained in the continuum. The chemical reaction network (CRN) of MEM is as follows:

$$\text{r1: } N + R \underset{k^{\text{off}}_{\text{NR}}}{\overset{\hat{k}^{\text{on}}_{\text{NR}}}{\rightleftharpoons}} NR, \quad \text{r2: } N + E \underset{k^{\text{off}}_{\text{NE}}}{\overset{k^{\text{on}}_{\text{NE}}}{\rightleftharpoons}} NE$$

$$\text{r3: } NR + E \underset{k^{\text{off}}_{\text{NRE}}}{\overset{k^{\text{on}}_{\text{NRE}}}{\rightleftharpoons}} NRE, \quad \text{r4: } NE + R \underset{k^{\text{off}}_{\text{NER}}}{\overset{k^{\text{on}}_{\text{NER}}}{\rightleftharpoons}} NRE$$

$$\text{r5: } NR, NE, NRE \xrightarrow{\delta} \emptyset$$

$$[R_{\text{TOT}}] = [R] + [NR] + [NRE] \tag{3}$$

Upon formation of NE, the species negatively regulate the NR forward rate constant $k^{\text{on}}_{\text{NR}}$ following a Hill equation as follows:

$$\hat{k}^{\text{on}}_{\text{NR}} = k^{\text{on}}_{\text{NR}} \left(\frac{K^{\text{n}}}{K^{\text{n}} + [NE]^{\text{n}}} \right) \tag{4}$$

where $k^{\text{on}}_{\text{NR}}$ is the basal NR production rate.

A.2 Steady state analysis for threshold dependent perceptron behavior

At steady state, $d/dt[NR] = d/dt[NE] = 0$. We ignore the term δ and assume that $k^{\text{off}}_{\text{NRE}} = k^{\text{off}}_{\text{NER}}$, $k^{\text{on}}_{\text{NRE}} = \gamma k^{\text{on}}_{\text{NE}}$, $k^{\text{on}}_{\text{NER}} = \gamma k^{\text{on}}_{\text{NR}}$, and $r = [R]/[E]$. From Eq. 1,

$$\begin{aligned} &\hat{k}^{\text{on}}_{\text{NR}}[N][R] + k^{\text{off}}_{\text{NRE}}[NRE] - k^{\text{off}}_{\text{NR}}[NR] - k^{\text{on}}_{\text{NRE}}[NR][E] = \\ &k^{\text{on}}_{\text{NE}}[N][E] + k^{\text{off}}_{\text{NER}}[NRE] - k^{\text{off}}_{\text{NE}}[NE] - k^{\text{on}}_{\text{NER}}[NE][R] \end{aligned}$$

Eliminating $k^{\text{off}}_{\text{NRE}}[NRE]$ and $k^{\text{off}}_{\text{NER}}[NRE]$, we get,

$$\begin{aligned} \hat{k}^{\text{on}}_{\text{NR}}[N][R] - k^{\text{on}}_{\text{NE}}[N][E] &= k^{\text{off}}_{\text{NR}}[NR] + k^{\text{on}}_{\text{NRE}}[NR][E] - k^{\text{off}}_{\text{NE}}[NE] - k^{\text{on}}_{\text{NER}}[NE][R] \\ &= [NR](k^{\text{off}}_{\text{NR}} + \gamma k^{\text{on}}_{\text{NE}}[E]) - [NE](k^{\text{off}}_{\text{NE}} + \gamma k^{\text{on}}_{\text{NR}}[R]) \end{aligned}$$

Applying feedback expression of $\hat{k}^{\text{on}}_{\text{NR}}$,

$$\frac{K^{\text{n}}k^{\text{on}}_{\text{NR}}}{K^{\text{n}}+[NE]^{\text{n}}}[N][R]-k^{\text{on}}_{\text{NE}}[N][E]=k^{\text{off}}_{\text{NR}}[NR]+k^{\text{on}}_{\text{NRE}}[NR][E]-k^{\text{off}}_{\text{NE}}[NE]-k^{\text{on}}_{\text{NER}}[NE][R]$$
$$=[NR](k^{\text{off}}_{\text{NR}}+\gamma k^{\text{on}}_{\text{NE}}[E])-[NE](k^{\text{off}}_{\text{NE}}+\gamma k^{\text{on}}_{\text{NR}}[R])$$

Making $[NR]$ the subject, and denoting the feedback expression as $K^{\text{n}}/(K^{\text{n}}+[NE]^{\text{n}})=\beta$

$$[NR]=\frac{\beta k^{\text{on}}_{\text{NR}}[N][R]-k^{\text{on}}_{\text{NE}}[N][E]+[NE](k^{\text{off}}_{\text{NE}}+\gamma k^{\text{on}}_{\text{NR}}[R])}{k^{\text{off}}_{\text{NR}}+\gamma k^{\text{on}}_{\text{NE}}[E]}$$
$$=\frac{\beta k^{\text{on}}_{\text{NR}}r[N]-k^{\text{on}}_{\text{NE}}[N]+[NE](\frac{k^{\text{off}}_{\text{NE}}}{[E]}+\gamma r k^{\text{on}}_{\text{NR}})}{\frac{k^{\text{off}}_{\text{NR}}}{[E]}+\gamma k^{\text{on}}_{\text{NE}}} \tag{5}$$

Assuming $\gamma k^{\text{on}}_{\text{NE}} \gg k^{\text{off}}_{\text{NR}}/[E]$ and $\gamma r k^{\text{on}}_{\text{NR}} \gg k^{\text{off}}_{\text{NE}}/[E]$, we finally get,

$$[NR]\approx\frac{\beta k^{\text{on}}_{\text{NR}}r[N]-k^{\text{on}}_{\text{NE}}[N]+[NE](\gamma r k^{\text{on}}_{\text{NR}})}{\gamma k^{\text{on}}_{\text{NE}}}$$

Here, $[NR]\geq 0$ as concentration is always non-negative. We can write,

$$\frac{\beta k^{\text{on}}_{\text{NR}}r[N]-k^{\text{on}}_{\text{NE}}[N]+[NE](\gamma r k^{\text{on}}_{\text{NR}})}{\gamma k^{\text{on}}_{\text{NE}}}\geq 0$$
$$\beta k^{\text{on}}_{\text{NR}}r+\frac{[NE]}{[N]}\gamma r k^{\text{on}}_{\text{NR}}\geq k^{\text{on}}_{\text{NE}}$$
$$k^{\text{on}}_{\text{NR}}(\beta r+\gamma r\frac{[NE]}{N})\geq k^{\text{on}}_{\text{NE}}$$
$$k^{\text{on}}_{\text{NR}}\geq \underbrace{\left(\frac{[N]}{\beta r[N]+\gamma r[NE]}\right)}_{\Omega}k^{\text{on}}_{\text{NE}}$$
$$k^{\text{on}}_{\text{NR}}\geq \Omega k^{\text{on}}_{\text{NE}} \tag{6}$$

Hence, we get the threshold condition:

$$[NR]\approx\begin{cases}(\beta k^{\text{on}}_{\text{NR}}r[N]-k^{\text{on}}_{\text{NE}}[N]+[NE](\gamma r k^{\text{on}}_{\text{NR}}))/\gamma k^{\text{on}}_{\text{NE}} & \text{if } k^{\text{on}}_{\text{NR}}\geq\Omega k^{\text{on}}_{\text{NE}}\\ 0 & \text{if } k^{\text{on}}_{\text{NR}}<\Omega k^{\text{on}}_{\text{NE}}\end{cases} \tag{7}$$

We can rewrite the above condition in terms of perceptron inputs and weights as follows:

$$[NR]\approx\begin{cases}(\beta k^{\text{on}}_{\text{NR}}r[N]-k^{\text{on}}_{\text{NE}}[N]+[NE](\gamma r k^{\text{on}}_{\text{NR}}))/\gamma k^{\text{on}}_{\text{NE}} & \text{if } w_1x_1+w_2x_2\geq\Omega w_0\\ 0 & \text{if } w_1x_1+w_2x_2<\Omega w_0\end{cases} \tag{8}$$

A.3 Experimental results

A.3.1 Parameter screen

The underlying mechanism of the MEM-model consists of negative regulation of NR formation rate ($k^{\text{on}}_{\text{NR}}$) by NE. Initially, the concentration of NR is restricted to a near-zero value until $k^{\text{on}}_{\text{NR}}$ reaches a threshold (Eq. 6), leading to the binary classification of inputs. However, the ReLU-like behavior is obtained for specific parameter combinations, rendering parameter dependency of the model. To explore this parameter dependency, we conduct a parameter screen to identify suitable parameter sets for which the species NR exhibits ReLU-like behavior. Our screen involves a set of criteria to detect perceptron-like behavior for any given parameter set (Fig. 4d). Efficacy of these steps is demonstrated using two of the previously studied models, namely the molecular sequestration model (Moorman et al., 2019) and the phosphorylation-dephosphorylation model (Samaniego et al., 2021). We utilize the following algorithms to detect a perceptron-like activation function from the steady state NR concentration of a model. The value of the variables tol, z and y are chosen based on the model parameters.

Algorithm 1 ReLU Detection

flag ← 0, num_zero ← 0
m ← max(NR)
for i←1 to length(NR) **do**
    if NR^i ≤ 0.02*m **then**
        num_zero ← num_zero + 1
    end if
end for
Coordinates a←(0.75,NR), b←(0.74,NR),
c←(1,NR), d←(0.99,NR)
g_1 ← gradient for points c,d
g_2 ← gradient for points a,b
$d \leftarrow g_1 - g_2$
if num_zero ≥ z *and* $0 \leq d \leq$ tol **then**
    flag ← 1
end if

Algorithm 2 Sigmoid Detection

flag ← 0, num_zero ← 0, num_one ← 0
m ← max(P)
for i←1 to length(P) **do**
    if P^i ≤ 0.02*m **then**
        num_zero ← num_zero + 1
    end if
end for
for j←1 to length(P) **do**
    if P^j ≥ 0.98*m **then**
        num_one ← num_one + 1
    end if
end for
if num_zero ≥ z *and* num_one ≥ y **then**
    flag ← 1
end if

A.3.2 DECISION BOUNDARY ANALYSIS

The MEM-perceptron takes two inputs x_1 and x_2 and three weights w_0, w_1, w_2. The weights w_1, w_2 are for the inputs x_1, x_2, respectively, whereas w_0 is the bias. In the MEM-perceptron, weights and inputs together form the intrinsic NR formation rate, which is modulated further by NE. As observed, NR subdivides the surface formed by the inputs (x_1, x_2) into two classes, class 0 (orange) and class 1 (blue) by forming a decision boundary (white). We then change the weights and bias and observe that decision boundary shifts congruently with the analytical decision boundary (Fig. 3c,d), defined for two inputs as: $x_2 = -(w_1/w_2)x_1 + (w_0/w_2)$, where (w_1/w_2) is the slope and (w_0/w_2) is the intercept from the y-axis (x_2) of the boundary line. However, a boundary deviation Δ between the analytical decision boundary and simulated decision boundary emerges when the bias (w_0) is changed (Fig. 3b). Interestingly, the deviation Δ is traceable for a change in w_0 through the dependency of NR concentration on n, R and E. Traceability of Δ is shown in Fig. 2a and remains subject to further investigation as part of our ongoing expansion of this work.

The MEM-perceptron shown in this work takes two positive weights (w_1, w_2). However, it can also be used with one positive weight and one negative weight. The design of the MEM-perceptron with positive-negative weights is given in Fig. 4b. The resulting decision boundary for positive-negative weights shows a similar characteristic as the perceptron with only the positive weights, however, the slope of the boundary is positive and follows the equation $x_2 = (w_1/w_2)x_1 + (w_0/w_2)$. The surface plots of the positive-negative weight version are not shown here for brevity.

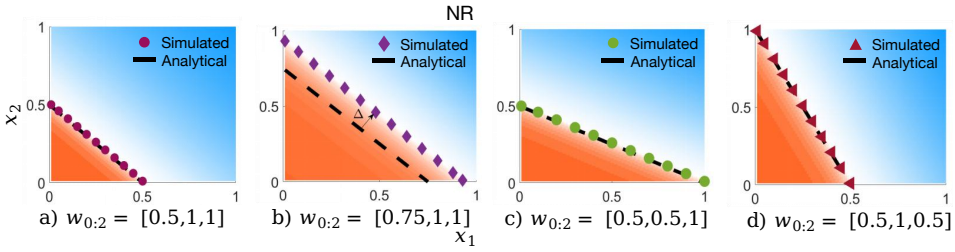

Figure 3: Concentration surface plots show decision boundaries corresponding to the weights. a,c-d) The analytical and simulated decision boundary lines align for the changing weights w_1 and w_2. b) Changing the bias w_0 causes a parallel deviation Δ of the simulated from the analytical line.

Table 1: Parameters used to generate the decision boundary in Fig. 3

Parameter	Value	Unit
$k_{\text{NR}}^{\text{on}}$	$[0.02, 2]$	$nM^{-1}s^{-1}$
$k_{\text{NE}}^{\text{on}}$	0.5	$nM^{-1}s^{-1}$
$k_{\text{NR}}^{\text{off}}$	0.005	s^{-1}
$k_{\text{NE}}^{\text{off}}$	0.005	s^{-1}
γ	10	dimensionless
$k_{\text{NRE}}^{\text{on}}$	5	$nM^{-1}s^{-1}$
$k_{\text{NER}}^{\text{on}}$	$[0.2, 20]$	$nM^{-1}s^{-1}$

Parameter	Value	Unit
$k_{\text{NRE}}^{\text{off}}$	0.005	s^{-1}
$k_{\text{NER}}^{\text{off}}$	0.005	s^{-1}
K	0.05	nM
n	6	dimensionless
R_{TOT}	7.85	nM
E	5	nM
δ	1	s^{-1}

A.4 Steady state Probability Approximation and Noise Measurement

The Chemical Master Equation (CME) (Van Kampen, 1992) captures the dynamic time evolution of interacting systems' joint probability distribution p(X, t). Here, $\mathbf{X}$ denotes the molecular count of each species S_i as $\mathbf{X} = [X_1, X_2 \dots X_N]^T$. The CME transforms the deterministic reaction rate constant of molecular interactions to the propensity function (Gillespie, 1976), which treats an interaction as a probabilistic event, with an expression as follows

$$\frac{d}{dt}p(x,t) = -\sum_i a_i(x,t)p(x,t) + \sum_i a_i(x-\nu_i,t)p(x-\nu_i,t) \tag{9}$$

where $a_i(x)$ is the propensity function that quantifies the state due to the occurrence of transition from state $\mathbf{X}$ to the next for reaction r_i. For steady state probability distribution, $p(x,t)_{ss}$, the time evolution of probability $p(x,t)$ can be represented as a system of linear equations:

$$\frac{d}{dt}p(x,t) = Sp(x,t) = Sp_{ss} \Rightarrow Sp_{ss} = 0 \text{ for steady-state} \tag{10}$$

To reduce the computational cost associated with the numerical approximation of CME for steady-state probability distribution, we treat CME as a system of linear equations for a truncated state-space $\hat{\Omega}$, elaborately outlined in Karim et al. (2012). In the truncated state-space $\hat{\Omega}$, the steady state probability distribution p_{ss} is approximated by transforming the normalization of probability as

$$\sum_{x\in\Omega} p_{ss} = 1 \text{ to } \sum_{x\in\hat{\Omega}} p_{ss} = 1 - \epsilon, \tag{11}$$

where ϵ is negligibly small, and the molecular strength of species $\mathbf{X}$ remains within a sufficiently large left (α) and right (β) boundary of the truncated state-space $\hat{\Omega} = \{\mathbf{X} : \alpha_i \leq X_i \leq \beta_i, \text{for all } i \leq N\}$. Finally, we use the coefficient of variation (CV) as a metric to compare the noise between a set of chemical reactions with and without the presence of exchanger molecules E, and is defined as below:

$$\text{CV} = \frac{\text{standard deviation of NR}}{\text{mean of NR}} = \frac{\sqrt{\text{variance of NR}}}{\text{mean of NR}} = \frac{\sigma_{\text{NR}}}{\mu_{\text{NR}}} \tag{12}$$

A.5 Biological Relevance of MEM

The dynamics which drives the decision making of the MEM-perceptron may relate to certain biophysical interactions, such as those seen in the synaptic cleft of neurons and in cellular pattern formation. In the synaptic cleft, regulators such as Glycine and D-serine (Papouin et al., 2012) bind to receptors to control neuronal activation and inhibition. The MEM-perceptron employs the likeliness of such physiological interactions and the roles similar to different regulators have been collectively attributed to a single type of regulator, which is the exchanger molecule E in the MEM model. Neurotransmitters directly bind to receptors and activate neurons similar to N and R forming NR in the MEM-model. On the other hand, neurotransmitters also bind with regulators to form an intermediate complex (Choquet & Triller, 2013) and the intermediate complex may couple with receptors forming a tripartite complex similar to NE and NRE respectively, as demonstrated in the MEM-model (Fig. 4a).

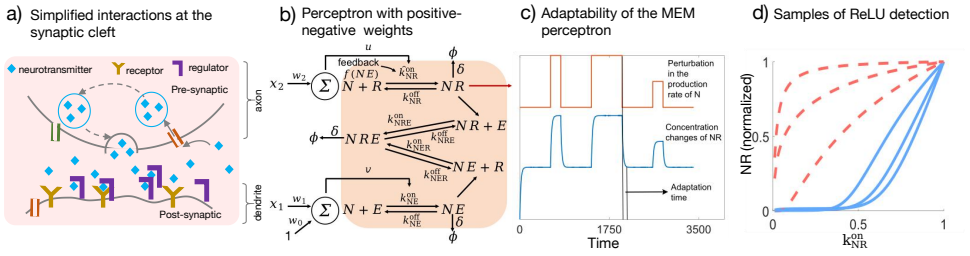

Figure 4: a) Interactions at the synaptic cleft (simplified) which serves as the inspiration for our design. b) Schematic diagram of the MEM perceptron with one positive weight and one negative weight. c) Adaptability of the MEM perceptron against perturbations of the concentration of N. d) Plot of some sample outputs of the ReLU detection algorithm. Blue lines (solid) are accepted. Orange lines (dashed) are rejected.